European Journal of Medicinal Chemistry 148 (2018): 372-383

DOI: https://doi.org/10.1016/j.ejmech.2018.02.009

Gold(III) bis(thiosemicarbazonate) compounds in breast cancer cells: cytotoxicity and thioredoxin reductase targeting

Vanessa Rodríguez-Fanjul,[a] Elena López-Torres,[b] M. Antonia Mendiola,[b] and Ana María Pizarro[a]*

[a] IMDEA Nanociencia, Faraday 9, 28049 Madrid, Spain.

[b] Departamento de Química Inorgánica, Universidad Autónoma de Madrid, Francisco Tomás y Valiente 7, 28049 Madrid, Spain.

*Correspondence should be addressed to A.M.P. (email: ana.pizarro@imdea.org).

ABSTRACT

Gold(III) compounds have received increasing attention in cancer research. Three gold complexes of general formula $[Au^{III}L]Cl$, where L is benzil bis(thiosemicarbazonate), L^1, (compound **1**), benzil bis(4-methyl-3-thiosemicarbazonate), L^2, (compound **2**), or benzil bis(4-cyclohexyl-3-thiosemicarbazonate), L^3, (compound **3**), have been synthesized and fully characterized, including the X-ray crystal structure of compound **3**, confirming square-planar geometry around the gold(III) centre. Compound **1** showed moderate cytotoxicity and accumulation in MCF7 breast cancer cells but did not inhibit thioredoxin reductase (TrxR) activity and did not induce reactive oxygen species (ROS) production. Compound **2**, the least cytotoxic, was found to be capable of modestly inhibiting TrxR activity and produced low levels of ROS in the MCF7 cell line. The most cytotoxic compound **3** had the highest cellular accumulation and its distribution pattern showed a clear preference for the cytosol and mitochondria of MCF7 cells. It readily hampered intracellular TrxR activity leading to a dramatic alteration to the cellular redox state and to the induction of cell death.

KEYWORDS

gold(III); thiosemicarbazones; thioredoxin reductase; cisplatin; reactive oxygen species

INTRODUCTION

Following the clinical success of auranofin for the treatment of rheumatoid arthritis, a number of gold(I) complexes have been investigated to treat a variety of diseases. In particular anticancer research has seen the successful early development of thiolate,[1, 2] phosphine,[3-6] NHC,[7-9] alkynyl,[10] and thiourea[11] gold(I) complexes.

Gold(III) compounds have inevitably received increasing attention as well. Gold(III) is isoelectronic with platinum(II), making gold(III) compounds attractive candidates in the development of cisplatin-inspired anticancer metallodrugs that overcome the clinical limitations of cisplatin, such as intrinsic and acquired resistance[12, 13] and diverse undesirable side effects such as neuro- and/or renal-toxicity or bone marrow-suppression.[14] However, gold(III) molecular mechanism to trigger cancer cell death has proved particularly intricate as a result of the metal's redox activity and its proneness to be reduced to gold(I/0) in the reducing environment of the tumour. Accompanying the $Au^{III}/Au^{I/0}$ intracellular redox chemistry, gold compounds are prone to undergo rapid ligand-exchange reactions, which additionally hinder the elucidation of their mechanism of action. Even so, an extraordinary effort from the labs of Messori, Fregona and Chi-Ming Che, among others,[15-24] have managed to outline a landscape of gold(III) possible targets, where gold–S/Se interactions play a major role. In this respect, two main systems have been identified as gold targets inside the cell; glutathione and thioredoxin.

Glutathione (GSH), a ubiquitous intracellular tri-peptide (γ-Glu-Cys-Gly), is the most abundant non-protein thiol present in animal cells. GSH plays an important role in many cellular processes, including detoxification of xenobiotics, maintenance of the intracellular redox balance

and thiol status, and modulation of cellular apoptosis, among others.[25-27] Many tumours exhibit increased GSH levels, which are associated with a proliferative response and drug resistance.[28]

Together with GSH, the thioredoxin system plays an essential role in cytoprotection and in signalling pathways involving reactive oxygen species (ROS). The thioredoxin system comprises the small redox protein thioredoxin (Trx), selenocysteine-containing thioredoxin reductase (TrxR) and NADPH, and acts as the cells' major antioxidant system through its disulfide reductase activity.[29-31] Thioredoxin reductase specifically reduces the oxidized Trx (Trx-S_2), turning it to a dithiol Trx–$(SH)_2$ using NADPH.[32] The Trx-$(SH)_2$ form is a strong disulfide reductase which keeps proteins in the reduced form and participates in the cell antioxidant response.[31] Mammalian cells express primarily two isoforms of TrxR; TrxR1 is found in the cytoplasm, and TrxR2 is located in the mitochondria. TrxR is highly expressed in many cancer cells, and this elevated expression is correlated with increased proliferation of tumours, inhibition of apoptosis, highly invasive and metastatic tumour activity and drug resistance.[33]

Finally, ROS are formed as a natural byproduct of the normal cellular metabolism of oxygen and are responsible for the maintenance of the redox homeostasis in cells.[34] ROS are thought to play a dual role in cell biology.[35] They act as mediators of intracellular signalling to regulate numerous physiological and biological responses when the amount of ROS is low and/or moderate.[36-40] Yet ROS also function as cellular damaging agents when an increase in ROS levels or a decrease in the cellular antioxidant capacity occurs, by damaging lipids, proteins, and DNA[41] and promoting carcinogenesis.[42]

Thiosemicarbazones (TSCs) and bis(thiosemicarbazones) have also attracted the attention of medicinal chemists in cancer research. Their anti-cancer activity has been mainly attributed to

the chelation of endogenous iron.[43-45] TSC metal complexes have been reported to show a diverse range of biological activity. In particular those of iron and copper have received much interest, followed by Ni(II), Zn(II) and even Cd(II) and Pd(II), regarding their antiproliferative effects.[46]

Here we report the antiproliferative activity of three square-planar gold(III) complexes. In an effort to stabilise the gold centre in its +3 oxidation state, we have employed a tetradentate bis(thiosemicarbazone) ligand that acts as a shell, protecting the central Au^{III} toward ligand substitution reactions, thereby lessening gold(III)'s vulnerability toward rapid intracellular reduction. The complexes are stable in dimethylsulfoxide solution over a week. The complexes present an intricate cytotoxic activity, likely to be due to a complex mechanism of action, which we have in part unravelled. Following reports implicating the GSH and the Trx systems in the cytotoxicity exerted by other families of gold complexes, we have probed the role of GSH by both depleting and over-producing it in MCF7 cells, and subsequently measuring the effect of such modulation on cell viability resulting from exposure to our compounds. Additionally, we have quantified the increase in ROS production triggered by our compounds in the breast cancer cell line by means of fluorescence microscopy and spectroscopy, and tried to relate such an effect to the inhibition of the seleno-enzyme TrxR. Intracellular accumulation and distribution studies have also contributed to outline the mechanism of action of this promising family of gold(III) metallodrugs.

RESULTS AND DISCUSSION

Synthesis of Gold(III) Complexes

The three complexes **1**, **2** and **3** (Chart 1), were synthesized in good yield by mixing a solution of $Na[AuCl_4]\cdot 2H_2O$ with the corresponding ligand in a 1:1 ligand to metal ratio at room temperature. In the case of the ligands bearing NH_2 and NHMe pendant groups, the addition of a base to the reaction medium facilitates the solubilisation of the ligand and the reaction evolves faster and with better yield. The addition of base is not necessary in the reaction of complex **3**, where the ligand bears a cyclohexyl group, since this reaction is carried out in dichloromethane, which readily dissolves the bezil bis(thiosemicarbazone) derivative.

Chart 1. Gold(III) Benzil Bis(thiosemicarbazonate) Complexes Studied in This Work.

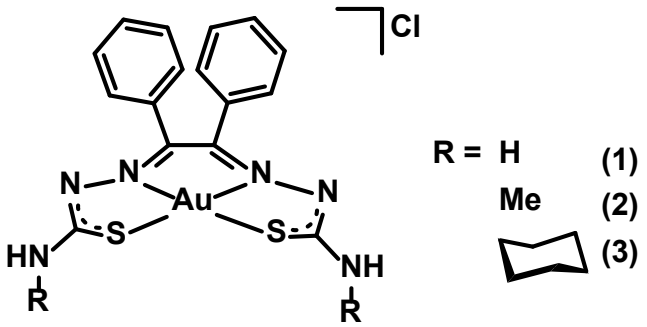

Compound	Formula	R
1	$[Au^{III}L^1]Cl$	H
2	$[Au^{III}L^2]Cl$	CH_3
3	$[Au^{III}L^3]Cl$	C_6H_{11}

The spectroscopic characterization of the three complexes reveals that all of them possess analogous structures. As can be confirmed by ^1H NMR and elemental analysis, in the three compounds the ligand is doubly deprotonated and there is a chloride as counterion, confirming

the tripositive oxidation state for gold. The mass spectra of the three complexes show the peak corresponding to $[M]^+$. In the three complexes the ^1H chemical shifts are different from those of the free ligands due to its coordination to the gold(III) centre. The ^{13}C NMR spectra show a strong shift of the signals corresponding to CN and CS groups, confirming the thiosemicarbazonate behaves as a N_2S_2 tetradentate ligand.

The three gold compounds were found to be strikingly stable in dimethylsulfoxide solution (Fig. S1). This observation is consistent with reports demonstrating that gold(III) bis(thiosemicarbazonates) forming five-membered chelates show extraordinary stability toward gold reduction and colloid formation, even in PBS buffer at pH 7.4 and 37 °C.[47]

X-ray Structure of Complex 3·C_7H_8, $[Au^{III}L^3]Cl·C_7H_8$

The asymmetric unit of complex **3·C_7H_8** is made up by two $[Au^{III}L^3]^+$ cations, two toluene molecules and two chlorides (Figure S2), the latter linked by strong hydrogen bonds (N–H···Cl distances in the range 2.21–2.39 Å; Figure S3 and Table S4). The two $[Au^{III}L^3]^+$ units do not show significant differences, except that one of the cyclohexyl groups in one of the cations is disordered into two positions. Only one of the cations is depicted in Figure 1. The Au^{III} ion is in a square-planar coordination environment provided by a doubly deprotonated ligand acting as a N_2S_2 chelate donor, a coordination mode that leads to the formation of three five-membered chelate rings conferring a high stability to the complex.

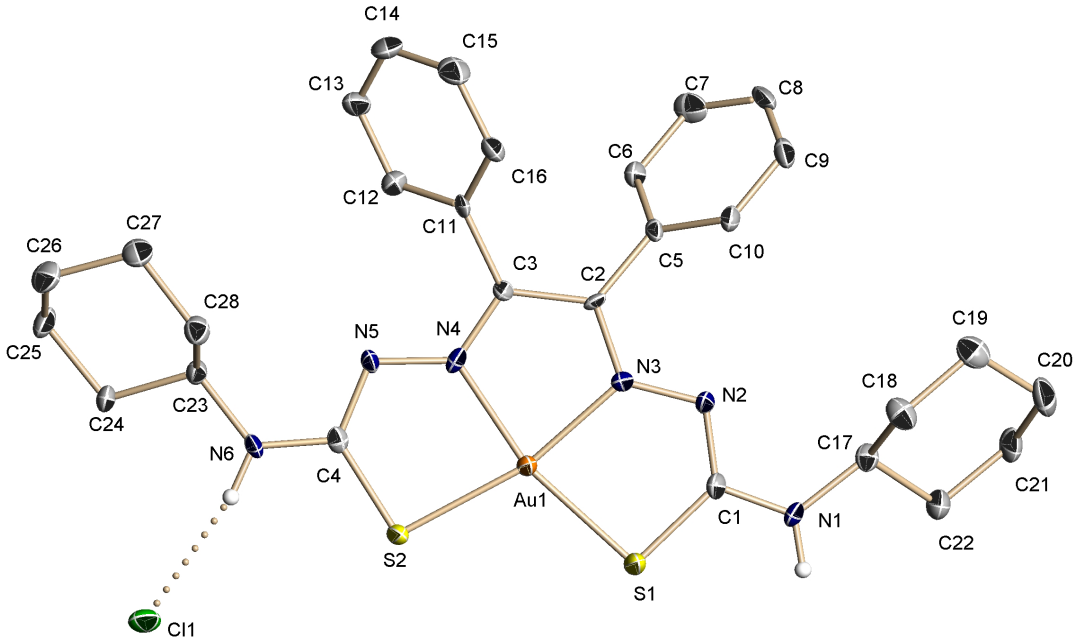

Figure 1. ORTEP representation (thermal ellipsoids drawn at 50% probability level), including atom numbering scheme, of one of the cations and one chloride present in the asymmetric unit of complex **3**·C_7H_8. Hydrogen atoms, except those of the amine groups, and toluene have been omitted for clarity. Detailed crystallographic data are shown in Tables S1–3 in the Supporting Information.

The bis(thiosemicarbazonate) skeleton is virtually planar with a maximum deviation from the least-square plane of 0.0834 Å for S1 in one of the cations and 0.0493 Å for S4 in the other and with the gold atoms lying in the ligands' planes (maximum deviations 0.010 and 0.055 Å for Au1 and Au2, respectively). The Au–N bond distances range from 1.991(9) to 2.002(8) Å, while the Au–S distances range from 2.276(3) to 2.288(3) Å. These distances are very similar to Au–N and Au–S bond distances found in the only two gold(III)-bis(thiosemicarbazonate) complexes reported hitherto in the literature.[47] The angles around the gold(III) centres deviate from 90º due to ligand demands, with the smallest close to 81º and the highest to 109º. Although ligand

deprotonation usually increases charge delocalization, the C–S bond distances are 1.767(10) and 1.782(10) Å, which is consistent with the ligands favouring the thiol conformation. Both the cations and the chlorides act as 2-connected nodes, leading to the formation of tetrameric aggregates (Figure S3).

Cytotoxicity of Au^{III} Compounds towards Breast Cell Lines

We initially evaluated the cytotoxic activity of the three Au^{III} complexes in comparison with cisplatin (CDDP) in three cell lines of breast cancer: the estrogen receptor positive, progesterone receptor positive and HER2 negative MCF7 cell line, the triple-negative MDA-MB-231 cell line, and normal breast epithelial immortalized MCF10A cells. IC_{50} values (concentration of drug required to inhibit cell growth by 50% compared to control), were calculated from the cell viability dose response curves obtained after 24 h drug treatment (+72 h cell recovery) using the SRB assay. As observed in Figure 2, Au^{III} complexes are, in general, more active in MCF10A cells. Compounds **1**, **2** and **3** showed similar tendencies in cytotoxicity towards the three cell lines follow the order **3** > **1** > **2**. Compound **3** is the most potent among the three tested complexes and have similar activity profile to CDDP in the three cell lines (IC_{50} of CDDP are 8.9 μM (MCF7), 7.1 μM (MDA-MB-231), and 4.8 μM (MCF10A)). The cytotoxicity of the three god(III) compounds against MCF7 cells show significant divergence between one another.

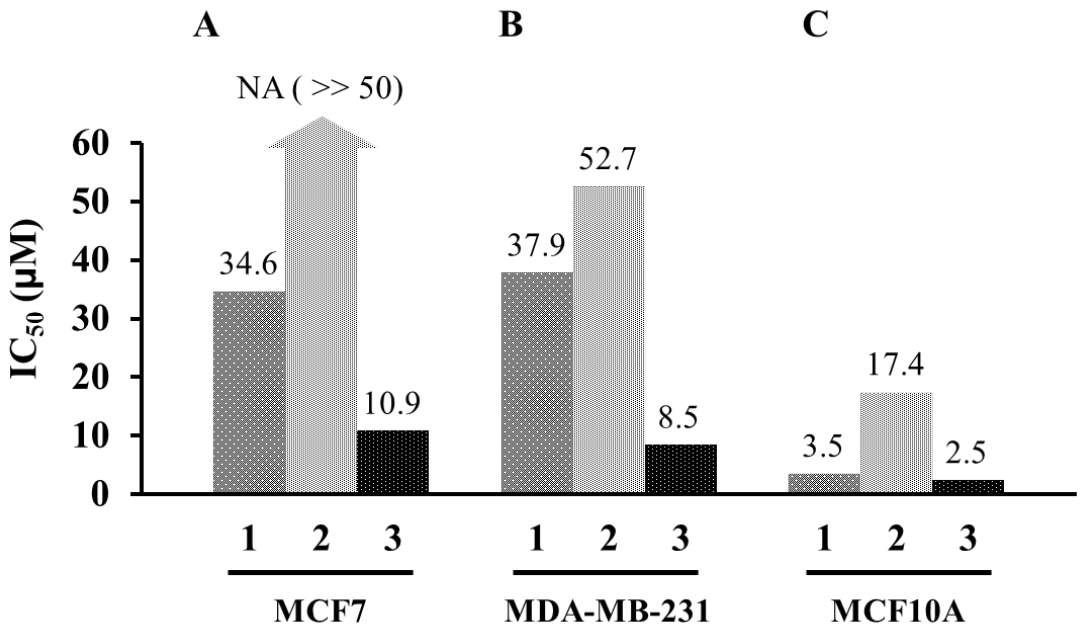

Figure 2. Antiproliferative activity of gold(III) complexes. Cell viability determined in MCF7 (A), MDA-MB-231 (B) and MCF10A (C) cells after 24 h of exposure to complexes **1**, **2** or **3** and allowed to recover for 72 h. CDDP was used as positive control (IC_{50} = 8.9 μM for MCF7, 7.1 μM for MDA-MB-231 and 4.8 μM for MCF10A cells). NA; not applicable.

Based on these data we selected the MCF7 cell line to carry out further studies in order to help us elucidate the root cause behind the observed differences in cytotoxicity and how it is related to the gold(III) compounds' mechanism to trigger cell death.

First, despite the robustness of our complexes toward ligand loss, nevertheless we investigated if Au^{III} compounds cytotoxicity in MCF7 cells was related to their free ligands activity. We compared the cytotoxic activity of compounds **1**, **2** and **3** with their correspondent free ligands in MCF7. Figure S4 shows IC_{50} values of 4.5, 2.6, and >>25 μM for free ligands L^1H_2, L^2H_2 and L^3H_2, respectively. Our data therefore indicate that cell viability inhibition is not related to that of their free ligands since their cytotoxic activity does not correlate, and is indeed the opposite of that of the corresponding metal complex. Since thiosemicarbazones appear to

exert their antitumour activity based on their ability to chelate essential iron, and subsequently halt cancer cell progression,[48] our results seem to indicate that gold hampers free TSC activity by clutching and stabilizing the bis(thiosemicarbazone) ligand, and that the [Au^{III}L[Cl compounds **1**–**3** exert a different mechanism of action. These results indirectly disregard rapid ligand loss, supporting the stability of our complexes in the biological media.

Metal Accumulation in MCF7 Cells

We evaluated the uptake of gold(III) complexes in order to determine whether the sensitivity of MCF7 cells to each Au^{III} compound correlates with intracellular gold accumulation. MCF7 cells were exposed to the Au^{III} complexes **1**, **2** and **3** at equimolar concentrations of 10 μM for 24 h, and total cellular accumulation of gold (net uptake between influx and efflux) was determined by Inductively Coupled Plasma Mass Spectrometry (ICP-MS). The highest intracellular levels of gold were observed after exposure to compound **3** (136.5 ± 11.1 ng Au/10^6 cells), followed by compound **1** (87.3 ± 4.0 ng Au/10^6 cells) and **2** (66.2 ± 4.6 ng Au/10^6 cells). The results are summarized in Figure 3. The cellular uptake values for compounds **1**, **2** and **3** are in accordance with their cell growth inhibitory potency, i.e., higher cytotoxicity correlates with higher intracellular accumulation.

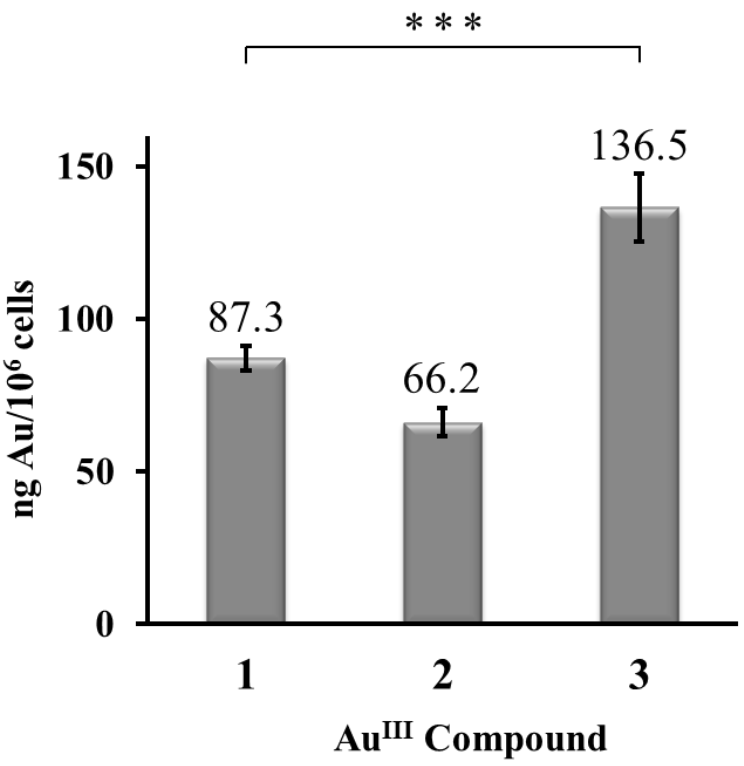

Figure 3. Cellular gold accumulation in the MCF7 breast cancer cell line. Drug-treatment period was 24 h with 10 μM Au^{III} complexes. Each value represents the mean ± CI (compound **1**, 87.3 ± 4.0 ng Au/10^6 cells; compound **2**, 66.2 ± 4.6 ng Au/10^6 cells; and compound **3**, 136.5 ± 11.1 ng Au/10^6 cells). All values were compared to the untreated controls and to one another for statistical significance calculations; $p<0.001$ for ***.

Effect of Modulation of Glutathione Cellular Levels on Au^{III}-Induced Cytotoxicity in MCF7 Cells

GSH acts as an antioxidant, a free radical scavenger and a detoxifying agent and plays an important role in the protection of cells against the toxic effects of a variety of compounds.[25] The latter include gold anticancer candidates, given the high affinity of gold for SH residues. Crucially GSH contains a thiol group in the cysteine residue, which favours the formation of GS–Au complexes.[49] We studied the effect of modulating intracellular levels of GSH on the

cytotoxicity caused by Au^{III} complexes **1**, **2** and **3** in MCF7 cells. We used two modulators of the availability of GSH at the intracellular level, L-buthionine-S,R-sulfoximine (LBSO) and N-acetyl-L-cysteine (NAC). Glutathione is synthesized from its constituent amino acids, glutamate, cysteine, and glycine, by the action of L-glutamate-cysteine ligase and glutathione synthetase.[25] LBSO is a GSH depletor since it inhibits selectively the enzyme L-glutamate-cysteine ligase.[50] NAC, conversely, is readily deacetylated in cells to yield L-cysteine thereby promoting intracellular GSH synthesis.[51] Table 1 and Figure 4 show that pre-treatment of MCF7 cells with a non-toxic dose of LBSO (50 μM; Figure S5A) significantly enhances the cytotoxicity of the three Au^{III} complexes (2-fold for compound **1,** 1.5-fold for **2**, and 7-fold for **3**, with respect to controls), whereas pre-treatment of cells with a non-toxic dose of NAC (500 μM; Figure S5B) almost completely suppressed induced-cell death by compounds **1** and **3** (not applicable for compound **2**). Results obtained from the co-treatment with the control compound (CDDP) showed a similar effect (Table S5 and Figure S6).

Table 1. Effect of LBSO (50 μM) and NAC (500 μM) in the Cytotoxicity of Au^{III} Complexes on the Growth of MCF7 Breast Cancer Cells.[a]

Treatment		IC_{50}[b] (μM), mean[c] ± CI		
LBSO	**NAC**	**1**	**2**	**3**
-	-	34.6 ± 5.2	NA (>> 50[d])	10.9 ± 0.5
+	-	14.9 ± 1.3	31.9 ± 2.4	1.5 ± 0.2
-	+	NA (>> 50[d])	NA (>> 50[d])	NA (>> 50[d])

[a] The drug treatment period was 24 h. Each value represents the mean ± CI of two to three independent experiments done in quadruplicate. All values were compared to the untreated controls and to one another for statistical significance calculations; $p < 0.001$. [b] IC_{50} is defined as the concentration of drug required to inhibit cell growth by 50% compared to control. [c] Goodness of fit monitored by 95% confidence intervals (CI). NA; not applicable. [d] IC_{50} is outside the range of the maximum concentration tested.

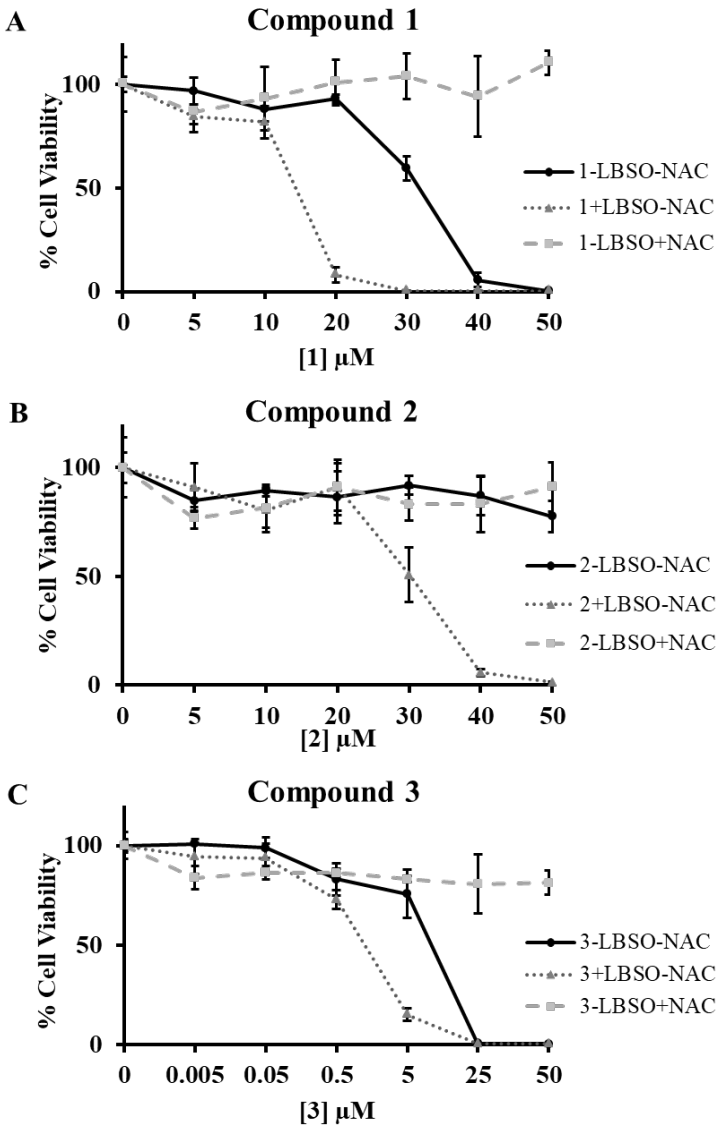

Figure 4. Effect of modulating the intracellular levels of GSH by pre-treatment with LBSO or NAC on the cytotoxicity caused by Au^{III} complexes in MCF7 cells. MCF7 cells were pre-treated with LBSO (50 µM) or NAC (500 µM) for 30 min followed by incubation with the indicated concentrations of compound **1** (A), **2** (B) and **3** (C) for 24 h at 37ºC. Data are representative of two to three independent experiments done in quadruplicate. Error bars represent the standard deviation.

The results indicate that intracellular GSH has an effect on the cytotoxic activity of all Au^{III} compounds in MCF7 cells, i.e.; higher levels of glutathione correspond to less cytotoxicity

exerted by the gold(III) compounds. The strongest effect on the cytotoxicity is observed for complex **3**, the most active of the series.

Gold-Induced ROS Production in MCF7 Cells

Given the protective role of a tetradentate ligand toward substitution reactions on a Au^{III} metal centre, we investigated other avenues than direct ligand substitution by GSH, that might relate the effect of GSH modulation to the cytotoxicity of our gold(III) compounds in an indirect manner. GSH plays a key role in protecting biological systems from ROS.[27] Based on our finding that GSH have strong influence on the activity of Au^{III} compounds **1**, **2** and **3** we explored if such effect could be related to the ability of these complexes to trigger ROS production.

We tested the levels of intracellular ROS induced after treatment of MCF7 cells by Au^{III} complexes using a fluorescein-labelled probe, DCF-DA. After being taken up by cells, the non-fluorescent DCF-DA is hydrolyzed by cellular esterases to dichlorodihydrofluorescin (DCFH), which is trapped within the cell. The non-fluorescent DCFH is then oxidized to fluorescent dichlorofluorescin (DCF) by action of cellular ROS. The DCF fluorescence intensity generated is directly proportional to ROS levels.[52, 53] Figure 5A shows that compound **1** did not trigger ROS production on MCF7 cells while treatment of MCF7 cells with compound **2** leads to a small increase in intracellular ROS production at the higher concentrations used (Figure 5B). In contrast, as shown in Figure 5C and Figure 6 (top), treatment of MCF7 cells with compound **3** induced strong ROS generation in a concentration-dependent manner. ROS levels were dramatically increased to a maximum level when the cells were treated with 10 μM of compound **3** (11.4-fold compared to control). These results were further confirmed by fluorescence microscopy (Figure 6, bottom). As control of ROS induction we treated MCF7 cells with 200

μM of LBSO or 6 mM of H_2O_2, and as negative control we treated the cells with 5 mM of NAC (Figure S7).

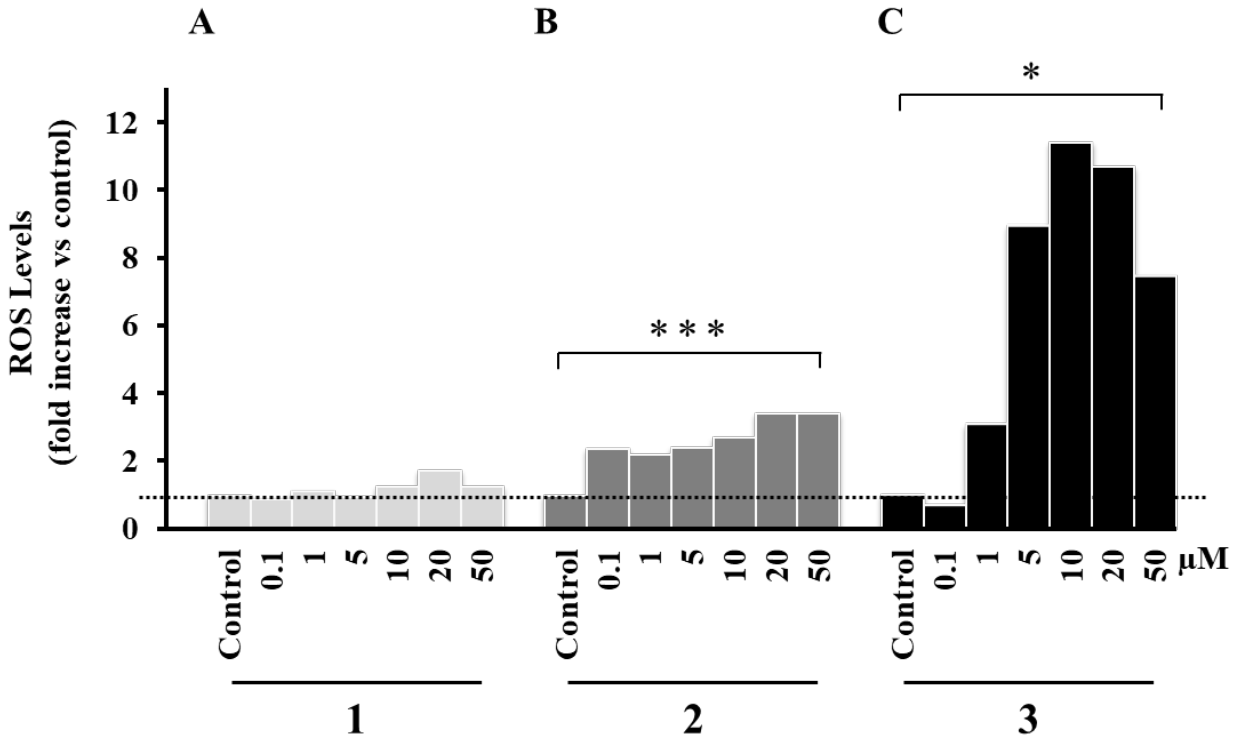

Figure 5. Induction of ROS by Au^{III} Complexes **1**, **2** and **3** in MCF7 cells. ROS levels in MCF7 cells after 90 min of incubation with Au^{III} compound **1** (A), **2** (B) or **3** (C) were measured by fluorescence spectroscopy after DCF-DA treatment. The results are expressed as the fold increase of cell fluorescence compared to control. All values were compared to the untreated controls and to one another for statistical significance calculations; $p<0.001$ for ***, and $p<0.05$ for *.

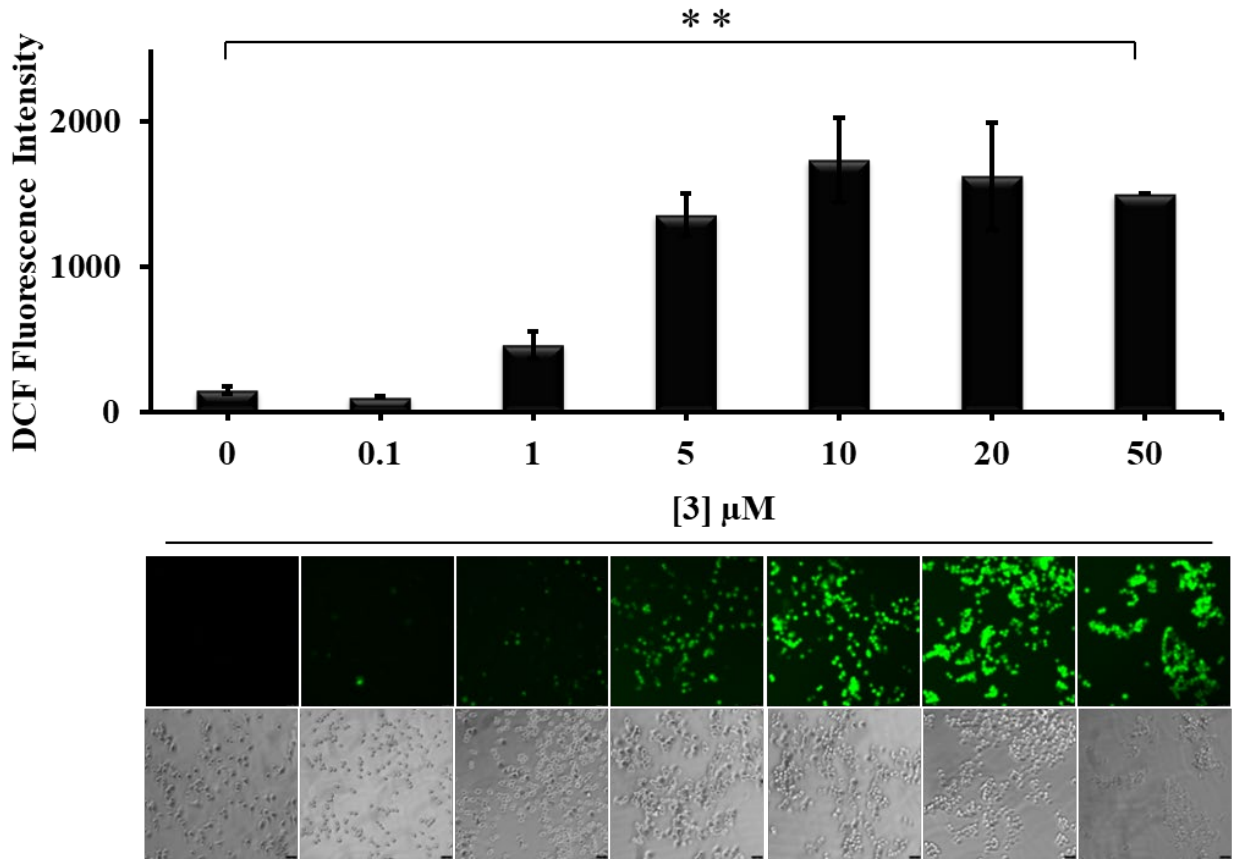

Figure 6. Induction of ROS in MCF7 cells. The MCF7 cells were treated with different concentrations of compound **3** for 90 min at 37ºC followed by the incubation with the fluorescence probe DCF-DA (20 µM) for 30 min. All values were compared to the untreated controls and among them for statistical significance calculations; $p < 0.01$ for **.The fluorescence images were acquired by inverted fluorescence microscopy. Scale bar: 50 µm.

In general, high amounts of ROS can induce macromolecular damage which can lead to apoptosis or necrosis.[34] However, low or optimum levels of ROS have beneficial effects on several physiological processes and play an important role in signalling pathways and maintenance of redox homeostasis promoting cell proliferation and cell survival.[54, 55]

Compound **1** showed moderate cytotoxicity towards MCF7 cells, which moderately increased with depleted levels of GSH, but did not induce ROS generation. This highlights the role of GSH and its chemoprotective effect overseeing intracellular metal homeostasis in the sensitivity of tumours to the cytotoxic effects of anticancer metal-based agents. Our data for compound **1** suggest a cell death mechanism that can be affected by GSH levels but is independent of Au^{III}-mediated ROS signalling.

Compound **2** was, however, non-toxic against MCF7 cells, and promoted only moderate increase on ROS levels. ROS are involved in interaction with critical signalling molecules to initiate proliferation, survival and differentiation such as MAP kinases, PI3 kinase, PTEN, NF-κB, HIFs and protein tyrosine phosphatases.[56, 57] Previous reports showed that low levels of ROS induce a transient activation of JNK signalling that promotes cell survival and anti-apoptotic signals.[54, 58] In addition, cancer stem cells (CSCs) show low intracellular ROS levels, which are required to maintain self-renewal, stemness, quiescence and an undifferentiated state and contribute to tumorigenesis.[59, 60] This protective effect of low/moderate ROS levels might explain why low production of ROS by compound **2** has little effect on hampering cell survival.

Finally, the imbalance due to excessive ROS production is known as oxidative stress.[36] Incapability of the cell to produce an effective antioxidant response results in damage to lipids, proteins and DNA. In particular, targeting redox homeostasis has recently been reviewed as an emerging plausible strategy for the treatment of breast cancer.[61-63] Our experimental results showed that compound **3** greatly increased total ROS production in MCF7 cells, correlating with the high cytotoxicity induced by this compound.

Inhibition of TrxR Activity by Au^{III} Compounds *in Vitro* and in MCF7 Cells

The Trx system is the other major thiol-dependent antioxidant system in mammalian cells; it controls ROS production and detoxification, maintaining redox intracellular balance. Several different classes of gold-based compounds (in both Au^{I} and Au^{III} oxidation states) are recognized as potent inhibitors of both cytosolic and mitochondrial TrxR.[64-66] TrxR catalyzes reduction of oxidized Trx by NADPH to the reduced active form Trx. Then, the redox active protein regulates the activity of several enzymes and protein substrates including those that counteract oxidative stress[67] and members of peroxiredoxin family that target the degradation of hydrogen peroxide.[68] Trx is also a potent singlet oxygen quencher and hydroxyl radical scavenger and so it can act directly on certain ROS.[69] In our aim to explain the differences in the gold-induced cytotoxicity and the mechanism of intracellular ROS accumulation upon exposure to **1**, **2** and **3**, we evaluated the TrxR activity in the test tube and also in MCF7 cells.

The effect of the gold(III) complexes on the activity of TrxR was measured by the dithiobis(nitrobenzoic acid) (DTNB) reduction assay using isolated rat liver TrxR.[70] The three Au^{III} complexes were found to cause a concentration-dependent inhibition of enzyme activity (in the test tube) as determined by the EC_{50} value (concentration of a drug where 50% of its maximal effect compared to control is observed). The EC_{50} values were 1.0 μM for compound **1**, 0.8 μM for compound **2** and 2.5 μM for compound **3** (Figure S8 and Table S6). The three Au^{III} complexes' inhibitory effects are similar and the EC_{50} values are lower than the IC_{50} dose obtained in the cytotoxic activity assay suggesting TrxR as a possible biological target for these Au^{III} compounds. Thus, we also determined the TrxR activity in MCF7 cells after gold(III) treatment (Table 2 and Figure S9).

Table 2. Inhibition of TrxR by Au^{III} Complexes in MCF7 Cell Lysates.[a]

EC_{50} (μM)		
1	**2**	**3**
NA (>10[b])	4.8	0.8

[a] The MCF7 cells were treated with different concentrations of the gold(III) complexes for 24 h at 37 ºC and lysed in lysis buffer. TrxR activity in the cell lysates was measured by the DTNB reduction assay. NA; not applicable. [b] EC_{50} is outside the range of the maximum concentration tested.

We observed that compound **1** inhibited only 25% of enzyme activity in MCF7 at the maximum concentration tested (10 μM), supporting the above notion that compound **1** induces cell death by a mechanism in which GSH is involved but independent of ROS signalling. Compound **2** induced a modest decrease in TrxR activity (EC_{50} = 4.8 μM), inhibiting the enzyme's activity moderately, which correlates with low induced levels of ROS and the non-cytotoxicity against MCF7 cells. Compound **3**, the most cytotoxic complex, induced a significant concentration-dependent inhibition of TrxR and the strongest inhibition in cells (EC_{50} = 0.8 μM) of the series. In good agreement with the results from the proliferation assay and GSH modulation, low concentrations of compound **3** strongly induced high cellular ROS levels and inhibited the activity of the redox relevant enzyme TrxR. Our data indicates that such an enzyme could be regarded as an effective molecular target of gold(III) compound **3**.

Gold Distribution in Cell Fractions

It has been widely reported that both cytosolic and mitochondrial TrxR are very specific targets of gold(III) complexes as they react mainly with thiol and/or selenol groups.[66] Gold(III) compounds AuTS and AuOAc are known to target TrxR1,[71] while mononuclear amidogold(III) complexes $[Au(dien)Cl]Cl_2$ (dien=2,2′-diethylendiamine), $[Au(py^{dmb}\text{-}H)(CH_3COO)_2]$ (py^{dmb}-

H=2-(1,1-dimethylbenzyl)-pyridine), [Au(bipy^{dmb}-H)(OH)]-(PF_6) (bipy^{dmb}-H=6-(1,1-dimethylbenzyl)-2,2′-bipyridine) and [Au(bipy^{dmb}-H)(2,6-xylidine)](PF_6), have been reported to target TrxR2.[72] Complexes [Au[DMDT)X_2] and [Au(ESDT)X_2] (DMDT = N,N-dimethyldithiocarbamato; ESDT = ethylsarcosinedithiocarbamato; X = Cl, Br) are reported to inhibit both cytosolic and mitochondrial TrxR.[19]

We described above that compound **3** strongly inhibited TrxR activity whereas compounds **1** and **2** had no or moderate effect on TrxR activity. Trx systems are not ubiquitously present in the cell, therefore we determined intracellular gold distribution upon exposure to MCF7 cells to investigate possible co-location of our Au^{III} compounds **1**–**3** with the selenocysteine-containing enzyme, to further support TrxR activity as a key element in the molecular mechanism responsible for gold-mediated cell death.

We incubated MCF7 cells at 37 °C for 24 h with 10 μM of each Au^{III} complex and separated them into mitochondrial, cytosolic and nuclei/membrane/particulate (N/M/P) fractions to relate intracellular distribution of gold to the endogenous cytosolic and mitochondrial TrxR activities. Table 3 and Figure 7 show that distribution of gold in the three fractions is similar for compounds **1** and **2**. Compound **1** accumulated mostly in the N/M/P fraction (97%), and only 3% in the cytosol and mitochondria fractions, which agrees with the poor inhibition of TrxR activity. Significant amounts of gold reached the N/M/P fraction for compound **2** and little was accumulated in the cytosol and mitochondria (6% overall), correlating with the slight TrxR activity inhibition observed for this compound in MCF7 cells. Notably, 23% of the overall gold uptake for compound **3** was accumulated in the cytosolic fraction, while up to 8% of gold was found in the mitochondria of the breast cancer cells. Our data shows that approximately a third of total accumulation of complex **3** locates in the mitochondrial and cytosolic fractions, in

comparison to 3 and 6% for compound **1** and **2**, respectively. These results seem to clarify the mechanism of action of complex **3**, further supporting TrxR as its molecular target. Even if the high accumulation of **3** in the cytosol could suggest a preference for TrxR1, the accumulated gold in the mitochondria is also extraordinarily high, suggesting that the interaction of **3** with TrxR2 might play a key role in the inhibition of the Trx system.

Table 3. Cellular Distribution of Au^{III} Complexes (as %ng Au/10^6 cells) in MCF7 Cells.[a]

Cellular Uptake (%ng Au/10^6 cells)			
Compound	**Mitochondria**	**Cytosol**	**N/M/P**
1	1	2	97
2	3	3	94
3	8	23	69

[a] Drug-treatment period was 24 h exposed to 10 μM Au^{III} complexes. The results are expressed as the percentage of elemental gold internalized in each fraction with respect to the total amount of gold internalized for each compound. All values were compared to the untreated controls and to one another for statistical significance calculations; $p<0.001$. N/M/P, nuclei/membrane/particulate fraction.

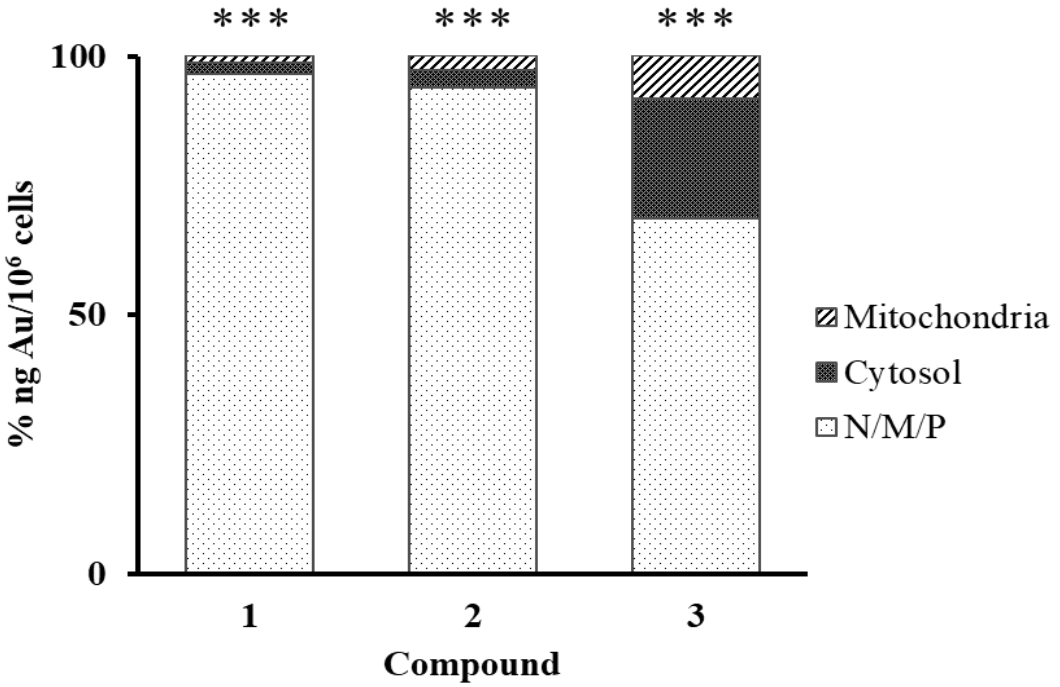

Figure 7. Cellular distribution of Au^{III} complexes (as %ng $Au/10^6$ cells) in MCF7 cells. Drug-treatment period was 24 h exposed to 10 μM Au^{III} compounds. The results are expressed as the percentage of ^{197}Au internalized from each fraction with respect to the total amount of ^{197}Au internalized for each compound. All values were compared to the untreated controls and to one another for statistical significance calculations; $p<0.001$ for ***.

CONCLUSION

The limited spectrum of activity, drug resistance, and side effects of cisplatin in cancer treatment have led to the search for other active transition metal complexes. In particular, complexes based on Au^{III}, isoelectronic to Pt^{II}, have received considerable interest. The goal of the present study was to synthesize, structurally characterize and biologically investigate a series of gold(III) bis(thiosemicarbazonate) complexes. The choice of the tetradentate chelating ligand appeared to be appropriate in order to retain optimal stability. The complexes studied in this work present different antiproliferative activities against cancerous and immortalized human breast cell lines. The cytotoxic activity against MCF7 cells of the gold(III) compounds reported here appear to exert distinct molecular mechanisms of action. Compound **1** did not inhibit TrxR activity and did not induce ROS formation but showed moderate cytotoxic activity in MCF7 cells. Increase in the synthesis of GSH induced by NAC, a promotor of GSH biosynthesis, suppressed cell death whereas depletion of GSH caused by LBSO, an inhibitor of GSH biosynthesis, led to an increase in its cytotoxicity. The highest proportion of gold was found in the nuclei/membrane/particulate fraction. These data put together indicates that compound **1** clearly behaves differently to **2** and **3** regarding the mechanism by which it hampers cell replication. Future work should pursue the possibility of cause direct DNA damage, proteasome inhibition, modulation of specific kinases, and other cellular processes that eventually trigger apoptosis. Modulation of intracellular GSH also affected the cytotoxicity of compound **2** towards MCF7 cells and only small amount of the total gold accumulation was found in the mitochondrial and cytosolic fractions. Additionally, compound **2** showed to be non-toxic towards MCF7 cells at the maximum concentration tested, inducing only a slight increase of ROS levels, a plausible result of a moderate inhibition of TrxR activity. Finally, compound **3** exhibited the

highest cytotoxic activity against MCF7 cells. The cytotoxicity correlates with GSH modulation, ROS production, and TrxR activity inhibition. Moreover, compound **3** was effectively accumulated in MCF7 cells and located in high amounts (31%) in the cytosol and in the mitochondria and therein induced ROS-dependent cell death by inhibition of TrxR activity. Compound **3**, with a cytotoxic potency similar to cisplatin, may be representing a new family of TrxR inhibitors for development in anticancer research.

EXPERIMENTAL SECTION

Methods and Instrumentation. Microanalyses were carried out using a LECO CHNS-932 Elemental Analyzer. Melting points were determined using Stuart™ Melting Point Apparatus SMP3 or an IA9100 Melting Point Apparatus (Electrothermal). IR spectra in the 4000-400 cm^{-1} range were recorded as KBr pellets on a Jasco FT/IR-410 spectrophotometer. FAB^+ mass spectra were recorded on a VG Auto Spec instrument using Cs as the fast atom and m-nitrobenzylalcohol (mNBA) as the matrix. ESI mass spectra in positive mode were recorded on a Q-STAR PULSAR I instrument using a hybrid analyzer QTOF (Quadrupole time-of-flight). ^1H, ^{13}C Bruker AVIII HD-300 MHz using DMSO-d_6 or $CDCl_3$ as solvent and TMS as internal reference.

Synthesis of the Compounds. All the chemicals were purchased from standard commercial sources such as ABCR and Sigma-Aldrich, and used without further purification.

All tested compounds, including cisplatin (Sigma-Aldrich, ≥99.9%), possess a purity of at least ≥95%, as determined by combustion analysis (all analyses were within ±0.4% of theoretical values).

Benzil bis(thiosemicarbazone), L^1H_2. Benzil bis(thiosemicarbazone) was prepared following a procedure previously reported.[73] Elemental analysis, calculated for $C_{16}H_{16}N_6S_2$: C, 53.91; H, 4.52; N, 23.58; S, 17.99. Found: C, 54.15; H, 4.49; N, 23.29; S, 18.09. Melting point, 240 °C. ^1H NMR (300 MHz, DMSO-d_6) δ 9.8 (s, 2H, NH), 8.6 (s, 2H, NH_2), 8.3 (s, 2H, NH_2), 7.7 (m, 4H, Ph), 7.4 (m, 6H, Ph). ^{13}C NMR (300 MHz, DMSO-d_6) δ 179.1 (CS), 140.5 (CN), 133.1, 130.1, 128.9, 126.8 (Ph). IR (KBr, cm^{-1}) 3420, 3386, 3342, 3330, 3210, 3151(s) [ν(NH)], 1608(s)

[δ(NH_2)], 1581(s) [ν(C=N)+thioamide II] and 848(w) [thioamide IV]. FAB^+ (m/z) 714.0 $[2M+H]^+$ (25%), 357.0 $[M+H]^+$ (100%).

Benzil bis(4-methyl-3-thiosemicarbazone), L^2H_2. This ligand was prepared following the procedure previously described.[74] Elemental analysis, calculated for $C_{18}H_{20}N_6S_2$: C, 56.22; H, 5.24; N, 21.86; S, 16.68. Found: C, 55.90; H, 5.24; N, 21.71; S, 16.49. Melting point, 224 °C. ^{1}H NMR (300 MHz, DMSO-d_6) δ 9.8 (s, 2H, NH), 8.9 (q, ^3J = 5.2 Hz, 2H, NH), 7.7 (m, 4H, Ph), 7.4 (m, 6H, Ph), 3.0 (d, ^3J = 4.5 Hz, 6H, CH_3). ^{13}C NMR (300 MHz, DMSO-d_6) δ 178.6 (CS), 140.4 (CN), 133.2, 130.3, 129.1, 126.8 (Ph), 31.5 (CH_3). IR (KBr, cm^{-1}): 3435(s) and 3335(s) [ν(NH)], 1601(w) [ν(C=N)], 1546(s) [thioamide II], 845(w) [thioamide IV]**.** FAB^+ (m/z) 769.6 $[2M+H]^+$ (10%), 385.2 $[M+H]^+$ (80%).

4-cyclohexyl-3-thiosemicarbazide. 4-cyclohexyl-3-thiosemicarbazide was prepared according to the procedure previously reported.[75]

Benzil bis(4-cyclohexyl-3-thiosemicarbazone), L^3H_2. A solution of benzil (1.50 g, 7.15 mmol) and 10 drops of HCl (conc.) in dry methanol (75 mL) was added to a solution of 4-cyclohexyl-3-thiosemicarbazide (2.47 g, 14.30 mmol) in the same solvent (125 mL) with 1 mL of HCl (conc.). The solution was stirred under reflux for 1 h and later overnight at room temperature. The pale yellow precipitate formed was filtered off, washed with methanol and vacuum dried (2.98 g, 80%). Elemental analysis, calculated for $C_{28}H_{36}N_6S_2$: C, 64.58; H, 6.97; N, 16.40; S, 12.31. Found: C, 64.71; H, 7.06; N, 16.23; S, 12.29. Melting point, 220 °C. ^{1}H NMR (300 MHz, $CDCl_3$) δ 8.62 (s, 2H, NH), 7.56 (6H, Ph, m), 7.34 (4H, Ph, m), 7.04 (d, ^3J = 8.4 Hz, NH), 4.12 (m, 2H, CH-Cy), 1.82 (m, 4H, Cy), 1.50-1.00 (m, 8H). ^{13}C NMR (300 MHz, $CDCl_3$) δ 175.9 (CS), 146.9 (CN), 130.1, 129.7, 129.3, 128.7 (Ph), 52.0 (CH-Cy), 31.8, 25.4, 23.8 (CH_2-Cy). IR

(KBr, cm^{-1}): 3344(s) and 3333(s) [ν(NH)], 1567(w) [ν(C=N)], 1521(s) [thioamide II], 872 [thioamide IV]. FAB^+ (m/z) 1041.2 $[2M+H]^+$ (10%), 521.2 $[M+H]^+$ (100%).

***Gold(III) benzil bis(thiosemicarbazonate) chloride,* 1**. A solution of 100 mg (0.28 mmol) of $Na[AuCl_4]\cdot 2H_2O$ in 3 mL of methanol was added to a solution of 98 mg (0.28 mmol) of benzil bis(thiosemicarbazone) and 23 mg (0.56 mmol) of $LiOH\cdot H_2O$ in 10 mL of the same solvent. The mixture was stirred for three hours at room temperature and the yellow precipitate formed was filtered off, washed with ethanol and vacuum dried (110 mg, 68%). Elemental analysis, calculated for $AuC_{16}H_{14}N_6S_2Cl$: C, 32.76; H, 2.40; N, 14.32; S, 10.90. Found: C, 32.54; H, 2.47; N, 14.39; S, 10.86. Melting point, 149 °C. ^{1}H NMR (300 MHz, DMSO-*d*$_6$) δ 7.79-7.08 (m, NH_2 + Ph). ^{13}C NMR (300 MHz, DMSO-*d*$_6$) δ 173.7 (CS), 153.7 (CN), 136.2, 129.9, 129.4, 129.1, 129.0, 128.8, 128.7, 128.0 (Ph). IR (KBr, cm^{-1}): 3344(m) and 3178(m) [ν(NH)], 1605(s) [δ(NH_2)+ν(C=N)], 1515(s) [thioamide II], 842(w) [thioamide IV]. ESI^+ (m/z) 553.1 $[M]^+$.

***Gold(III) benzil bis(4-methyl-3-thiosemicarbazonate) chloride,* 2**. This complex was obtained following the same procedure described for the synthesis of **1** but adding 106 mg (0.28 mmol) of 4-methyl-3-thiosemicarbazone (green, 140 mg, 82%). Elemental analysis, calculated for $AuC_{18}H_{18}N_6S_2Cl$: C, 35.15; H, 2.95; N, 13.67; S, 10.41. Found C, 34.88; H, 3.02; N, 13.60; S, 10.32. Melting point, 178 °C. ^{1}H NMR (300 MHz, DMSO-*d*$_6$) δ 9.64 (br s, 2H, NH), 7.76 (m, 2H, Ph), 7.55 (m, 2H, Ph), 7.38 (m, 6H, Ph) 3.15 (br s, 3H, CH_3). ^{13}C NMR (300 MHz, DMSO-*d*$_6$) δ 163.3, 163.2 (CS), 149.9, 149.8 (CN), 134.4, 134.1, 131.0, 130.5, 129.4, 129.2, 128.0, 127.0 (Ph), 31.6, 31.5 (CH_3). IR (KBr, cm^{-1}): 3370(s) [ν(NH)], 1577(s) [ν(C=N)+thioamide II], 831(w) [thioamide IV**].** ESI^+ (m/z) 579.08 $[M]^+$, 963.22 $[Au(L^2)_2]^+$, 1159.17 $[2M]^+$.

***Gold(III) benzil bis(4-cyclohexyl-3-thiosemicarbazonate) chloride,* 3**. To a solution of 100 mg (0.19 mmol) of L^3H_2 in 8 mL of DCM was added 70 mg (0.19 mmol) of $Na[AuCl_4]\cdot 2H_2O$ solved in 2 mL of ethanol. The solution formed was stirred for three hours at room temperature. The solvent was removed until a dark green solid was formed, which was filtered, washed with small portions of cold DCM and dried under vacuum (127 mg, 88%). Elemental analysis, calculated for $AuC_{28}H_{34}N_6S_2Cl$: C, 44.76; H, 4.56; N, 11.19; S, 8.52. Found: C, 44.51; H, 4.60; N, 10.93; S, 8.65. Melting point, 151 °C. ^{1}H NMR (300 MHz, DMSO-d_6) δ 7.99-7.05 (m, 12H, Ph+NH), 3.96 (br s, 2H, CH-Cy), 2.40-0.75 (m, 20H, CH_2-Cy]. ^{13}C NMR (300 MHz, $CDCl_3$) δ 173.9 (CS), 155.1 (CN), 130.7, 130.5, 129.7, 128.8, 128.2, 127.7 (Ph), 60.2 (CH-Cy), 32.1, 25.1, 24.5 (CH_2-Cy). IR (KBr, cm^{-1}): 3334(s) [ν(NH)], 1562(s), 1521(s) [thioamide II], 862(w) [thioamide IV]. ESI^+ (m/z) 715.20 $[M]^+$. Slow evaporation of a solution in DCM/toluene (1/1) afforded crystals suitable for single crystal X-ray diffraction.

X-ray Diffraction. Data for compound $3\cdot C_7H_8$ were acquired using a Bruker Kappa Apex-II diffractometer equipped with an Apex-II CCD area detector using a graphite monochromator (Mo K_α radiation, λ = 0.71073 Å). The substantial redundancy in data allows empirical absorption corrections (SADABS)[76] to be applied using multiple measurements of symmetry-equivalent reflections. The raw intensity data frames were integrated with the SAINT program, which also applied corrections for Lorentz and polarization effects.[77] The software package SHELXTL version 6.10 was used for space group determination, structure solution and refinement. The structures were solved by direct methods (SHELXS-97),[78] completed with difference Fourier syntheses, and refined with full-matrix least squares using SHELXL-2014 minimizing $\omega(F_0^2 - F_c^2)$. Weighted R factors (R_w) and all goodness of fit S are based on F^2; conventional R factors (R) are based on F.[79] All non-hydrogen atoms were refined with

anisotropic displacement parameters. C–H hydrogen atoms were placed onto calculated positions and refined riding on their parent atom. Those on nitrogen where located in a difference Fourier map, but they were also placed onto calculated positions. All scattering factors and anomalous dispersions factors are contained in the SHELXTL 6.10 program library. One of the cyclohexyl groups is disordered into two positions. This disorder could be modelled but the H atom of the CH group could not be neither located in the difference Fourier map nor satisfactorily located onto its calculated position, so it is omitted from the model although is considered in the formula.

CCDC 1587069 contains the supplementary crystallographic data for this paper. These data can be obtained free of charge from the Cambridge Crystallographic Data Centre via www.cdcc.cam.ac.uk/data_request/cif.

Cell Culture. The human MCF7 breast cancer cell line was obtained from American Type Culture Collection (ATCC) and maintained in Dulbecco's modified Eagle's medium (DMEM) Low Glucose (LabClinics) supplemented with 10% foetal bovine serum (Gibco, Life Technologies), 1% of 2 mM GlutaMAX-I (Gibco, Life Technologies) and 1% penicillin/streptomycin (VWR). MDA-MB-231 breast cancer cell line was purchased from ATCC and cultured in DMEM High Glucose (LabClinics) supplemented with 10% foetal bovine serum, 1% of 2 mM GlutaMAX-I and 1% penicillin/streptomycin. MCF10A epithelial breast cell line was obtained from ATCC and maintained in HuMEC Basal Serum Free Medium (GIBCO) supplemented with HuMEC Supplement (GIBCO), Bovine Pituitary Extract (GIBCO) and 1% penicillin/streptomycin.

All cell lines were grown as adherent monolayers at 37 °C in a 5% CO_2 humidified atmosphere and subcultured at approximately 70−80% confluency. Experiments were conducted on exponentially growing cells.

Exposure to Au^{III} Compounds. Stock solutions of the Au^{III} complexes were first prepared by dissolving compound **1**, **2** or **3** in 100% sterile DMSO to assist dissolution and in order to obtain a concentration of 4 mM and stored at -20 ºC. The exact concentration was confirmed by ICP-MS and then diluted into 0.9% saline and medium. Prior to all treatments, the cells were allowed to adhere for 24 or 48 h and then exposed to test compounds. For cell viability curves, cells were exposed to 0.005−50 μM test compounds for 24 h. For cellular accumulation and distribution studies, Au^{III} complexes were tested at 10 μM for 24 h. All experiments were performed in parallel with DMSO vehicle control. Cisplatin, a metal-based cytotoxic agent used to treat various types of cancers, was used as a positive control in all assays.

Cellular Cytotoxicity. For the evaluation of cellular cytotoxicity, 5000 cells were seeded in 96-well plates (VWR) and grown for 48 h in complete medium. Solutions of the Au^{III} compounds were prepared and added to the wells to obtain a final concentration ranging from 0 to 50 μM, and the cells were incubated for 24 h at 37ºC. Following 24 h of drug exposure, cells were washed with PBS (Fisher Scientific), supplied with fresh medium, and allowed to grow for 72 h. Then, the protein content (proportional to living cells in culture) was measured using the Sulforhodamine B (SRB) assay[80] using a UV-visible spectrophotometer (Sinergy H4 microplate reader) at 510 nm. The percentage of surviving cells was calculated from the ratio of absorbance of treated to untreated cells (control cells). The IC_{50} value was calculated as the concentration reducing the proliferation of the cells by 50% and is presented as a mean ± CI of two to three independent experiments of four replicates each.

Cellular Accumulation in MCF7 Cells. MCF7 cells were seeded at a density of 1.5 x 10^6 cells/100 mm Petri dish in 9 mL of culture medium (three dishes were prepared per compound tested, and three untreated control dishes) and incubated for 24 h at 37 ºC. After 24 h of incubation, cells were exposed to the Au^{III} complexes. Solutions of the Au^{III} compounds were prepared by diluting a freshly prepared stock solution (in DMSO) of the corresponding complex in 0.9% saline and medium to a final concentration of 10 μM. After 24 h of drug exposure at 37 ºC on a 5% CO_2 incubator, the drug-containing medium was removed, and the cells were washed with PBS, trypsinized, and counted using a hemocytometer. The cells were centrifuged, eliminated the media, and stored at -20 ºC until digestion for ICP-MS analysis for ^{197}Au content. These experiments were all carried out in triplicate.

Gold Distribution in MCF7 Cells. Cell pellets were obtained as described above, and were fractionated using the Mitochondria Isolation Kit for Cultured Cells from Thermo Scientific according to the supplier's instructions. The cells fractions (N/M/P: nuclei/membrane/particulate fraction, C: cytosol and M: mitochondria) were stored at -20ºC until digestion for ICP-MS analysis for ^{197}Au content. These experiments were all carried out in triplicate.

ICP-MS Analysis. The cell pellets were digested as described below. To the cell pellets 0.3 mL of freshly distilled 70% HNO_3 (Sigma Aldrich) were added, and the samples were transferred into Wheaton V-Vials with a PTFE-faced rubber-lined cap (Sigma Aldrich). The vials were heated in an oven at 80 ºC for 16 h to fully digest the samples and allowed to cool. Then each sample was transferred to a tube of 15 mL. 0.3 mL of freshly 37% HCl (Sigma Aldrich) were added to each tube for metal stabilization. Doubly deionised water was then added to afford a maximum final concentration of 5% HNO_3 (suitable for ICP-MS analysis) prior to quantification of ^{197}Au.

In Vitro TrxR Activity Assays

TrxR Activity Assay by DTNB Assay. To determine the inhibition of TrxR an established microplate reader based assay was performed with minor modifications. For this purpose, commercially available Thioredoxin Reductase Assay Kit (Sigma-Aldrich) was used. In this assay, TrxR catalyzes the reduction of 5,5´-dithiobis (2-nitrobenzoic) acid (DTNB) with NADPH to 5-thio-2-nitrobenzoic acid (TNB), which produces a strong yellow colour, which is measured at 412 nm.[29] The compounds were freshly dissolved at various concentrations in 0.9% saline and medium from the stock solutions prepared in DMSO. Aliquots (3 μL) of the enzyme solution were added to each 47 μL of potassium phosphate buffer pH 7.0 containing the Au^{III} compounds in graded concentrations or vehicle (DMSO) without compounds (control probe), in a 96-well plate. The resulting solutions were incubated for 90 min (shaking every 30 min) at 37 ºC. Then, a master mixture in potassium phosphate buffer pH 7.0 and 50 mM EDTA containing DTNB and NADPH was added (final concentration: 2 mM and 240 μM, respectively). After proper mixing, the formation of TNB was monitored with a microplate reader (Sinergy H4 microplate reader) at 412 nm in 31 s intervals for 10 min. The increase in TNB concentration over time followed a linear trend, and the enzymatic activities were calculated as the slopes (increase in absorbance per second) thereof. For each tested compound, the non-interference with the assay components was confirmed by a negative control experiment using an enzyme-free solution. The EC_{50} values were calculated as the concentration of compound decreasing the enzymatic activity of the untreated control by 50% and are given as the means and error of two or three repeated experiments in triplicate or quadruplicate.

TrxR Activity Assay in Cell Lysates. Cells were treated with various concentrations of the Au^{III} complexes for 24 h at 37 ºC and then, they were harvested and washed twice with phosphate-

buffered saline (PBS). Total cellular proteins were extracted with a mixture of RIPA Buffer (Thermo Scientific) and Protease Inhibitor Cocktail (MedChem Express) for 5 min on ice and subsequent scraping. The total protein content was quantified using the Pierce BCA Protein Assay Kit (Thermo Scientific). TrxR activity in cell lysates was measured by the DTNB assay. Briefly, the cell extract containing 92 μg of total proteins was incubated in a final reaction volume of 50 μL containing potassium phosphate buffer pH 7.0 for 90 min (shaking every 30 min) at 37 ºC. The reaction was started by addition of NADPH and DNTB, and then the TrxR activity was detected by measurement of TNB quantity at 412 nm as described above.

Intracellular ROS Determination by the DCFDA Assay. 50,000 MCF7 cells per well were seeded in a 24-well plate and allowed to adhere for 24 h at 37 ºC. 200 μL per well of serial dilutions of different Au^{III} complexes in medium were added to obtain the required final test concentrations of Au^{III} compounds (0–50 μM). Immediately after 90 minutes of exposure to Au^{III} complexes at 37 ºC, the ROS indicator DCF-DA (20 μM) was added to each well, and incubation continued for 30 min at 37 ºC in the dark. The fluorescence was then measured on a spectrofluorometer at λ_{ex} = 485 nm and λ_{em} = 535 nm. The fluorescence induction factor (fold) for each concentration of Au^{III} compounds was calculated by dividing the reading of each well by the average reading of the negative control (0 μM). The cells were also visualized and photographed under a Leica inverted fluorescence microscope.

Statistical Analysis. All statistical analysis was performed using R Statistical Software (version 3.3.2 (2016-10-31); R Foundation for Statistical Computing, Vienna, Austria) by one-way analysis of variance (**ANOVA**) (*$p<0.05$, **$p<0.01$, and ***$p<0.001$).

ASSOCIATED CONTENT

Supporting Information

The Supporting Information for this manuscript includes crystallographic data in CIF format, and supporting figures and tables.

AUTHOR INFORMATION

Corresponding Authors

*E-mail: **ana.pizarro@imdea.org**

Author Contributions

AMP and ELT designed the research; ELT and MAM synthesized and characterized the complexes and ELT performed the crystal structure resolution and analysis; VRF performed the biological experiments and analyzed the data. The manuscript was written through contributions of all authors. All authors have given approval to the final version of the manuscript.

Notes

The authors declare no competing financial interest.

ACKNOWLEDGMENTS

Dr. A. Arnáiz is gratefully acknowledged for assistance in the Cell Culture Unit at IMDEA Nanociencia. This research was supported by the EC (FP7-PEOPLE-2013-CIG, no. 631396), the MINECO of Spain (RYC-2012-11231, and CTQ2014-60100-R), the Instituto de Salud Carlos III (PS09/00963), and the Comunidad Autónoma de Madrid (S2013/MIT-2850).

REFERENCES

(1) Kamei, H.; Koide, T.; Kojima, T.; Hashimoto, Y.; Hasegawa, M. Effect of Gold on Survival of Tumor-Bearing Mice. *Cancer Biother. Radiopharm.* **1998**, *13*, 403-406.

(2) Stallings-Mann, M.; Jamieson, L.; Regala, R. P.; Weems, C.; Murray, N. R.; Fields, A. P. A Novel Small-Molecule Inhibitor of Protein Kinase Cι Blocks Transformed Growth of Non–Small-Cell Lung Cancer Cells. *Cancer Res.* **2006**, *66*, 1767-1774.

(3) Berners-Price, S. J.; Mirabelli, C. K.; Johnson, R. K.; Mattern, M. R.; McCabe, F. L.; Faucette, L. F.; Sung, C.; Mong, S.; Sadler, P. J.; Crooke, S. T. In Vivo Antitumor Activity and In Vitro Cytotoxic Properties of bis[1,2-bis(Diphenylphosphino)Ethane]gold(I) Chloride. *Cancer Res.* **1986**, *46*, 5486-5493.

(4) Pillarsetty, N.; Katti, K. K.; Hoffman, T. J.; Volkert, W. A.; Katti, K. V.; Kamei, H.; Koide, T. In Vitro and in Vivo Antitumor Properties of Tetrakis((Trishydroxy-Methyl)Phosphine)Gold(I) Chloride. *J. Med. Chem.* **2003**, *46*, 1130-1132.

(5) Tian, S.; Siu, F.; Kui, S. C. F.; Lok, C.; Che, C. M. Anticancer Gold(I)-Phosphine Complexes as Potent Autophagy-Inducing Agents. *Chem. Commun.* **2011**, *47*, 9318-9320.

(6) Ott, I.; Qian, X.; Xu, Y.; Vlecken, D. H. W.; Marques, I. J.; Kubutat, D.; Will, J.; Sheldrick, W. S.; Jesse, P.; Prokop, A.; Bagowski, C. P. A Gold(I) Phosphine Complex Containing a Naphthalimide Ligand Functions as a TrxR Inhibiting Antiproliferative Agent and Angiogenesis Inhibitor. *J. Med. Chem.* **2009**, *52*, 763-770.

(7) Hickey, J. L.; Ruhayel, R. A.; Barnard, P. J.; Baker, M. V.; Berners-Price, S. J.; Filipovska, A. Mitochondria-Targeted Chemotherapeutics: The Rational Design of Gold(I) N-Heterocyclic Carbene Complexes That Are Selectively Toxic to Cancer Cells and Target Protein Selenols in Preference to Thiols. *J. Am. Chem. Soc.* **2008**, *130*, 12570-12571.

(8) Rubbiani, R.; Kitanovic, I.; Alborzinia, H.; Can, S.; Kitanovic, A.; Onambele, L. A.; Stefanopoulou, M.; Geldmacher, Y.; Sheldrick, W. S.; Wolber, G.; Prokop, A.; Wölfl, S.; Ott, I. Benzimidazol-2-Ylidene Gold(I) Complexes Are Thioredoxin Reductase Inhibitors with Multiple Antitumor Properties. *J. Med. Chem.* **2010**, *53*, 8608-8618.

(9) Zou, T.; Lum, C.; Lok, C.; To, W.; Low, K.; Che, C. M. A Binuclear Gold(I) Complex with Mixed Bridging Diphosphine and Bis(N-Heterocyclic Carbene) Ligands Shows Favorable

Thiol Reactivity and Inhibits Tumor Growth and Angiogenesis In Vivo. *Angew. Chem. Int. Ed.* **2014**, *53*, 5810-5814.

(10) Meyer, A.; Bagowski, C. P.; Kokoschka, M.; Stefanopoulou, M.; Alborzinia, H.; Can, S.; Vlecken, D. H. W.; Sheldrick, W. S.; Wölfl, S.; Ott, I. On the Biological Properties of Alkynyl Phosphine Gold(I) Complexes. *Angew. Chem. Int. Ed.* **2012**, *51*, 8895-8899.

(11) Yan, K.; Lok, C.; Bierla, K.; Che, C. M. Gold(I) Complex of N,N[Prime or Minute]-Disubstituted Cyclic Thiourea With In Vitro and In Vivo Anticancer Properties-Potent Tight-Binding Inhibition of Thioredoxin Reductase. *Chem. Commun.* **2010**, *46*, 7691-7693.

(12) Siddik, Z. H. Cisplatin: Mode of Cytotoxic Action and Molecular Basis of Resistance. *Oncogene* **2003**, *22*, 7265-7279.

(13) Galluzzi, L.; Senovilla, L.; Vitale, I.; Michels, J.; Martins, I.; Kepp, O.; Castedo, M.; Kroemer, G. Molecular Mechanisms of Cisplatin Resistance. *Oncogene* **2012**, *31*, 1869-1883.

(14) Florea, A. M.; Busselberg, D. Cisplatin as an Anti-Tumor Drug: Cellular Mechanisms of Activity, Drug Resistance and Induced Side Effects. *Cancers* **2011**, *3*, 1351-1371.

(15) Messori, L.; Abbate, F.; Marcon, G.; Orioli, P.; Fontani, M.; Mini, E.; Mazzei, T.; Carotti, S.; O'Connell, T.; Zanello, P. Gold(III) Complexes as Potential Antitumor Agents: Solution Chemistry and Cytotoxic Properties of Some Selected Gold(III) Compounds. *J. Med. Chem.* **2000**, *43*, 3541-3548.

(16) Gabbiani, C.; Mastrobuoni, G.; Sorrentino, F.; Dani, B.; Rigobello, M. P.; Bindoli, A.; Cinellu, M. A.; Pieraccini, G.; Messori, L.; Casini, A. Thioredoxin Reductase, an Emerging Target for Anticancer Metallodrugs. Enzyme Inhibition by Cytotoxic Gold(III) Compounds Studied with Combined Mass Spectrometry and Biochemical Assays. *MedChemComm* **2011**, *2*, 50-54.

(17) Gamberi, T.; Massai, L.; Magherini, F.; Landini, I.; Fiaschi, T.; Scaletti, F.; Gabbiani, C.; Bianchi, L.; Bini, L.; Nobili, S.; Perrone, G.; Mini, E.; Messori, L.; Modesti, A. Proteomic Analysis of A2780/S Ovarian Cancer Cell Response to the Cytotoxic Organogold(III) Compound Aubipy(c). *J. Proteomics* **2014**, *103*, 103-120.

(18) Milacic, V.; Chen, D.; Ronconi, L.; Landis-Piwowar, K. R.; Fregona, D.; Dou, Q. P. A Novel Anticancer Gold(III) Dithiocarbamate Compound Inhibits the Activity of a Purified 20S Proteasome and 26S Proteasome in Human Breast Cancer Cell Cultures and Xenografts. *Cancer Res.* **2006**, *66*, 10478-10486.

(19) Saggioro, D.; Rigobello, M. P.; Paloschi, L.; Folda, A.; Moggach, S. A.; Parsons, S.; Ronconi, L.; Fregona, D.; Bindoli, A. Gold(III)-Dithiocarbamato Complexes Induce Cancer Cell Death Triggered by Thioredoxin Redox System Inhibition and Activation of ERK Pathway. *Chem. Biol.* **2007**, *14*, 1128-1139.

(20) Lum, C. T.; Wai-Yin Sun, R.; Zou, T.; Che, C.-M. Gold(III) Complexes Inhibit Growth of Cisplatin-Resistant Ovarian Cancer in Association with Upregulation of Proapoptotic PMS2 Gene. *Chem. Sci.* **2014**, *5*, 1579-1584.

(21) Chow, K. H.-M.; Sun, R. W.-Y.; Lam, J. B. B.; Li, C. K.-L.; Xu, A.; Ma, D.-L.; Abagyan, R.; Wang, Y.; Che, C.-M. A Gold(III) Porphyrin Complex with Antitumor Properties Targets the Wnt/β-Catenin Pathway. *Cancer Res.* **2010**, *70*, 329-337.

(22) Warzajtis, B.; Glisic, B. D.; Savic, N. D.; Pavic, A.; Vojnovic, S.; Veselinovic, A.; Nikodinovic-Runic, J.; Rychlewska, U.; Djuran, M. I. Mononuclear Gold(III) Complexes with L-Histidine-Containing Dipeptides: Tuning the Structural and Biological Properties by Variation of the N-terminal Amino Acid and Counter Anion. *Dalton Trans.* **2017**, *46*, 2594-2608.

(23) Fung, S. K.; Zou, T.; Cao, B.; Lee, P.-Y.; Fung, Y. M. E.; Hu, D.; Lok, C.-N.; Che, C.-M. Cyclometalated Gold(III) Complexes Containing N-Heterocyclic Carbene Ligands Engage Multiple Anti-Cancer Molecular Targets. *Angew. Chem.* **2017**, *129*, 3950-3954.

(24) Jürgens, S.; Scalcon, V.; Estrada-Ortiz, N.; Folda, A.; Tonolo, F.; Jandl, C.; Browne, D. L.; Rigobello, M. P.; Kühn, F. E.; Casini, A. Exploring the C^N^C Theme: Synthesis and Biological Properties of Tridentate Cyclometalated Gold(III) Complexes. *Biorg. Med. Chem.* **2017**, *25*, 5452-5460.

(25) Lu, S. C. Regulation of Glutathione Synthesis. *Mol. Aspects Med.* **2009**, *30*, 42-59.

(26) Franco, R.; Cidlowski, J. A. Apoptosis and Glutathione: Beyond an Antioxidant. *Cell Death Differ.* **2009**, *16*, 1303-1314.

(27) Toledano, M. B.; Huang, M. E. The Unfinished Puzzle of Glutathione Physiological Functions, an Old Molecule That Still Retains Many Enigmas. *Antioxid. Redox Signal.* **2017**, *27*, 1127-1129.

(28) Jardim, B. V.; Moschetta, M. G.; Leonel, C.; Gelaleti, G. B.; Regiani, V. R.; Ferreira, L. C.; Lopes, J. R.; Zuccari, D. A. Glutathione and Glutathione Peroxidase Expression in Breast Cancer: an Immunohistochemical and Molecular Study. *Oncol. Rep.* **2013**, *30*, 1119-1128.

(29) Holmgren, A.; Bjornstedt, M. Thioredoxin and Thioredoxin Reductase. *Methods Enzymol.* **1995**, *252*, 199-208.

(30) Lu, J.; Holmgren, A. The Thioredoxin Antioxidant System. *Free Radical Biol. Med.* **2014**, *66*, 75-87.

(31) Arner, E. S.; Holmgren, A. The Thioredoxin System in Cancer. *Semin. Cancer Biol.* **2006**, *16*, 420-426.

(32) Lee, S.; Kim, S. M.; Lee, R. T. Thioredoxin and Thioredoxin Target Proteins From Molecular Mechanisms to Functional Significance. *Antioxid. Redox Signal.* **2013**, *18*, 1165-1207.

(33) S., A. E.; Holmgren, A. Physiological Functions of Thioredoxin and Thioredoxin Reductase. *Eur. J. Biochem.* **2000**, *267*, 6012-6019.

(34) Circu, M. L.; Aw, T. Y. Reactive Oxygen Species, Cellular Redox Systems, and Apoptosis. *Free Radic. Biol. Med.* **2010**, *48*, 749-762.

(35) Dickinson, B. C.; Chang, C. J. Chemistry and Biology of Reactive Oxygen Species in Signaling or Stress Responses. *Nat. Chem. Biol.* **2011**, *7*, 504-511.

(36) Schieber, M.; Chandel, N. S. ROS Function in Redox Signaling and Oxidative Stress. *Curr. Biol.* **2014**, *24*, R453-R462.

(37) Finkel, T. Signal Transduction by Reactive Oxygen Species. *J. Cell Biol.* **2011**, *194*, 7-15.

(38) Drogue, W. Free Radicals in the Physiological Control of Cell Function. *Physiol. Rev.* **2002**, *82*, 47-95.

(39) Sena, L. A.; Chandel, N. S. Physiological Roles of Mitochondrial Reactive Oxygen Species. *Mol. Cell* **2012**, *48*, 158-167.

(40) Holmstrom, K. M.; Finkel, T. Cellular Mechanisms and Physiological Consequences of Redox-dependent Signalling. *Nat. Rev. Mol. Cell Biol.* **2014**, *15*, 411-421.

(41) Cross, C. E.; Halliwell, B.; Borish, E. T.; Pryor, W. A.; Ames, B. N.; Saul, R. L.; McCord, J. M.; Harman, D. Oxygen Radicals and Human Disease. *Ann. Intern. Med.* **1987**, *4*, 526-545.

(42) Trachootham, D.; Alexandre, J.; Huang, P. Targeting Cancer Cells by ROS-mediated Mechanisms: a Radical Therapeutic Approach? *Nat. Rev. Drug Discov.* **2009**, *8*, 579-591.

(43) Serda, M.; Kalinowski, D. S.; Rasko, N.; Potuckova, E.; Mrozek-Wilczkiewicz, A.; Musiol, R.; Małecki, J. G.; Sajewicz, M.; Ratuszna, A.; Muchowicz, A.; Golab, J.; Simunek, T.; Richardson, D. R.; Polanski, J. Exploring the Anti-Cancer Activity of Novel

Thiosemicarbazones Generated Through the Combination of Retro-Fragments: Dissection of Critical Structure-Activity Relationships. *PLoS One* **2014**, *9*, 1-15.

(44) Akladios, F. N.; Andrew, S. D.; Parkinson, C. J. Cytotoxic Activity of Expanded Coordination bis-Thiosemicarbazones and Copper Complexes Thereof. *J. Biol. Inorg. Chem.* **2016**, *21*, 931-944.

(45) Kalinowski, D. S.; Quach, P.; Richardson, D. R. Thiosemicarbazones the New Wave in Cancer Treatment. *Future Med. Chem.* **2009**, *1*, 1143–1151.

(46) Beraldo, H.; Gambino, D. The Wide Pharmacological Versatility of Semicarbazones, Thiosemicarbazones and Their Metal Complexes. *Mini Rev. Med. Chem.* **2004**, *4*, 31-39.

(47) Bottenus, B. N.; Kan, P.; Jenkins, T.; Ballard, B.; Rold, T. L.; Barnes, C.; Cutler, C.; Hoffman, T. J.; Green, M. A.; Jurisson, S. S. Gold(III) bis-Thiosemicarbazonato Complexes: Synthesis, Characterization, Radiochemistry and X-Ray Crystal Structure Analysis. *Nucl. Med. Biol.* **2010**, *37*, 41-49.

(48) Whitnall, M.; Howard, J.; Ponka, P.; Richardson, D. R. A Class of Iron Chelators with a Wide Spectrum of Potent Antitumor Activity that Overcomes Resistance to Chemotherapeutics. *Proc. Natl. Acad. Sci. U. S. A.* **2006**, *103*, 14901-14906.

(49) Zou, T.; Lum, C. T.; Lok, C.-N.; Zhang, J.-J.; Che, C.-M. Chemical Biology of Anticancer Gold(III) and Gold(I) Complexes. *Chem. Soc. Rev.* **2015**, *44*, 8786-8801.

(50) Griffith, O. W. Mechanism of Action, Metabolism, and Toxicity of Buthionine Sulfoximine and its Higher Homologs, Potent Inhibitors of Glutathione Synthesis. *J. Biol. Chem.* **1982**, *257*, 13704-13712.

(51) Atkuri, K. R.; Mantovani, J. J.; Herzenberg, L. A.; Herzenberg, L. A. N-Acetylcysteine- a Safe Antidote for Cysteine/Glutathione Deficiency. *Curr. Opin. Pharm.* **2007**, *7*, 355-359.

(52) Mahalingaiah, P. K.; Singh, K. P. Chronic Oxidative Stress Increases Growth and Tumorigenic Potential of MCF-7 Breast Cancer Cells. *PLoS One* **2014**, *9*, e87371.

(53) Eruslanov, E.; Kusmartsev, S. Identification of ROS Using Oxidized DCFDA and Flow-Cytometry. In *Advanced Protocols in Oxidative Stress II*; Armstrong, D., Eds; Humana Press: Totowa, NJ, 2010; pp 57-72.

(54) Trachootham, D.; Lu, W.; Ogasawara, M. A.; Nilsa, R. D.; Huang, P. Redox Regulation of Cell Survival. *Antioxid. Redox Signal.* **2008**, *10*, 1343-1374.

(55) Boonstra, J.; Post, J. A. Molecular Events Associated with Reactive Oxygen Species and Cell Cycle Progression in Mammalian Cells. *Gene* **2004**, *337*, 1-13.

(56) Di Meo, S.; Reed, T. T.; Venditti, P.; Victor, V. M. Role of ROS and RNS Sources in Physiological and Pathological Conditions. *Oxid. Med. Cell. Longev.* **2016**, *2016*, 1245049.

(57) Ray, P. D.; Huang, B. W.; Tsuji, Y. Reactive Oxygen Species (ROS) Homeostasis and Redox Regulation in Cellular Signaling. *Cell. Signal.* **2012**, *24*, 981-990.

(58) Nakano, H.; Nakajima, A.; Sakon-Komazawa, S.; Piao, J. H.; Xue, X.; Okumura, K. Reactive Oxygen Species Mediate Crosstalk Between NF-KappaB and JNK. *Cell Death Differ.* **2006**, *13*, 730-737.

(59) Zhou, D.; Shao, L.; Spitz, D. R. Reactive Oxygen Species in Normal and Tumor Stem Cells. *Adv. Cancer Res.* **2014**, *122*, 1-67.

(60) Maraldi, T.; Angeloni, C.; Giannoni, E.; Sell, C. Reactive Oxygen Species in Stem Cells. *Oxid. Med. Cell. Longev.* **2015**, *2015*, 159080.

(61) Hecht, F.; Pessoa, C. F.; Gentile, L. B.; Rosenthal, D.; Carvalho, D. P.; Fortunato, R. S. The Role of Oxidative Stress on Breast Cancer Development and Therapy. *Tumour Biol.* **2016**, *37*, 4281-4291.

(62) Deng, Y. T.; Huang, H. C.; Lin, J. K. Rotenone Induces Apoptosis in MCF-7 Human Breast Cancer Cell-Mediated ROS Through JNK and p38 Signaling. *Mol. Carcinog.* **2010**, *49*, 141-151.

(63) Hsieh, C. J.; Kuo, P. L.; Hsu, Y. C.; Huang, Y. F.; Tsai, E. M.; Hsu, Y. L. Arctigenin, a Dietary Phytoestrogen, Induces Apoptosis of Estrogen Receptor-Negative Breast Cancer Cells Through the ROS/p38 MAPK Pathway and Epigenetic Regulation. *Free Radical Biol. Med.* **2014**, *67*, 159-170.

(64) Rigobello, M. P.; Scutari, G.; Folda, A.; Bindoli, A. Mitochondrial Thioredoxin Reductase Inhibition by Gold(I) Compounds and Concurrent Stimulation of Permeability Transition and Release of Cytochrome c. *Biochem. Pharmacol.* **2004**, *67*, 689-696.

(65) Cox, A. G.; Brown, K. K.; Arner, E. S.; Hampton, M. B. The Thioredoxin Reductase Inhibitor Auranofin Triggers Apoptosis Through a Bax/Bak-Dependent Process that Involves Peroxiredoxin 3 Oxidation. *Biochem. Pharmacol.* **2008**, *76*, 1097-1109.

(66) Bindoli, A.; Rigobello, M. P.; Scutari, G.; Gabbiani, C.; Casini, A.; Messori, L. Thioredoxin Reductase: A Target for Gold Compounds Acting as Potential Anticancer Drugs. *Coord. Chem. Rev.* **2009**, *253*, 1692-1707.

(67) Tonissen, K. F.; Di Trapani, G. Thioredoxin System Inhibitors as Mediators of Apoptosis for Cancer Therapy. *Mol. Nutr. Food Res.* **2009**, *53*, 87-103.

(68) Rhee, S. G.; Chae, H. Z.; Kim, K. Peroxiredoxins: a Historical Overview and Speculative Preview of Novel Mechanisms and Emerging Concepts in Cell Signaling. *Free Radic. Biol. Med.* **2005**, *38*, 1543-1552.

(69) Das, K. C.; Das, C. K. Thioredoxin, a Singlet Oxygen Quencher and Hydroxyl Radical Scavenger: Redox Independent Functions. *Biochem. Biophys. Res. Commun.* **2000**, *277*, 443-447.

(70) Hill, K. E.; McCollum, G. W.; B., R. F. Determination of Thioredoxin Reductase Activity in Rat Liver Supernatant. *Anal. Biochem.* **1997**, *253*, 123-125.

(71) Omata, Y.; Folan, M.; Shaw, M.; Messer, R. L.; Lockwood, P. E.; Hobbs, D.; Bouillaguet, S.; Sano, H.; Lewis, J. B.; Wataha, J. C. Sublethal Concentrations of Diverse Gold Compounds Inhibit Mammalian Cytosolic Thioredoxin Reductase (TrxR1). *Toxicol. In Vitro* **2006**, *20*, 882-890.

(72) Pia Rigobello, M.; Messori, L.; Marcon, G.; Agostina Cinellu, M.; Bragadin, M.; Folda, A.; Scutari, G.; Bindoli, A. Gold Complexes Inhibit Mitochondrial Thioredoxin Reductase: Consequences on Mitochondrial Functions. *J. Inorg. Biochem.* **2004**, *98*, 1634-1641.

(73) López-Torres, E.; Mendiola, M. A.; Pastor, C. J.; Souto Pérez, B. Versatile Chelating Behavior of Benzil bis(Thiosemicarbazone) in Zinc, Cadmium, and Nickel Complexes. *Inorg. Chem.* **2004**, *43*, 5222-5230.

(74) Calatayud, D. G.; Escolar, F. J.; López-Torres, E.; Mendiola, M. A. Facile and Selective Synthesis of 4-Methyl- and 4-Phenylthiosemicarbazide (=N-Methyl- and N-Phenylhydrazinecarbothioamide) Derivatives of Benzil (=1,2-Diphenylethane-1,2-dione). *Helv. Chim. Acta* **2007**, *90*, 2201-2216.

(75) Gonzalez-Garcia, C.; Mata, A.; Zani, F.; Mendiola, M. A.; Lopez-Torres, E. Synthesis and Antimicrobial Activity of Tetradentate Ligands Bearing Hydrazone and/or Thiosemicarbazone Motifs and Their Diorganotin(IV) Complexes. *J. Inorg. Biochem.* **2016**, *163*, 118-130.

(76) Sheldrick, G. M. *SADABS*, Version 2.03; Universität Gättingen: Göttingen, Germany, 1997-2001.

(77) Sheldrick, G. M. *SAINT+NT*, Version 6.04; Bruker AXS: Madison, WI, 1997-2001.

(78) Sheldrick, G. M. *SHELXTL*, Version 6.10; Bruker AXS: Madison, WI, 2000.

(79) Sheldrick, G. M. Phase Annealing in SHELX-90: Direct Methods for Larger Structures. *Acta Crystallogr. A* **1990**, *46*, 467-473.

(80) Vichai, V.; Kirtikara, K. Sulforhodamine B Colorimetric Assay for Cytotoxicity Screening. *Nat. Protoc.* **2006**, *1*, 1112-1116.